High resolution selective reflection spectroscopy as a probe of long-range surface interaction : measurement of the surface van der Waals attraction exerted on excited Cs atoms

Martine Chevrollier, Michèle Fichet, Marcos Oria, Gabriel Rahmat, Daniel Bloch, Martial Ducloy

Classification
Physics Abstracts
42.50 — 32.70J — 34.90

High resolution selective reflection spectroscopy as a probe of long-range surface interaction : measurement of the surface van der Waals attraction exerted on excited Cs atoms

Martine Chevrollier, Michèle Fichet, Marcos Oria, Gabriel Rahmat (*), Daniel Bloch and Martial Ducloy

Laboratoire de Physique des Lasers (**), Université Paris-Nord, Av. J. B. Clément, 93430 Villetaneuse, France

(*Received 27 January 1992, accepted 30 January 1992*)

Résumé. — La spectroscopie de réflexion sélective à l'interface d'une vapeur résonnante de faible densité, combinée à une technique de modulation de fréquence, permet de sonder à haute résolution et sans effet Doppler des atomes en interaction avec une surface. On analyse différents types d'interaction de surface envisageables, en insistant sur les conséquences spectroscopiques d'une attraction de surface de type van der Waals en z^{-3} (z : distance atome-surface). On présente en détail les résultats de deux séries d'expériences effectuées à l'interface entre une fenêtre diélectrique et la vapeur de Cs, excitée soit sur sa première raie de résonance $6S_{1/2}$-$6P_{3/2}$ (λ = 852 nm) soit sur la seconde raie de résonance 6S-7P (λ = 455 nm ou 459 nm). L'analyse des formes de raie obtenues dans une étude en pression démontre que la prise en compte de l'attraction van der Waals de surface est nécessaire à l'interprétation des déplacements de résonance et des fortes distortions de raie. Les forces d'attraction sont évaluées respectivement à 2 kHz μm^3 et 20 kHz μm^3 et paraissent indépendantes de la composante hyperfine choisie. On déduit également les paramètres d'élargissement et de déplacement collisionnels, pour des densités où la vapeur est déjà opaque. On discute les prédictions théoriques pour la force de l'attraction van der Waals, établies à partir des paramètres atomiques théoriques. Les valeurs prédites sont environ deux fois plus faibles que celles évaluées expérimentalement. La validité du calcul semble pécher dans la prise en compte de la nature diélectrique de l'interface, en particulier lorsque celle-ci devient opaque pour les fréquences correspondantes aux transitions atomiques virtuelles impliquées dans l'attraction van der Waals.

Abstract. — Selective reflection spectroscopy at an interface with a low-density resonant vapor, especially when combined with a frequency modulation technique, is a high-resolution Doppler-free tool for probing atoms interacting with a surface. We analyze different types of relevant surface interaction, emphasizing the spectral consequences of a van der Waals surface attraction associated to a z^{-3} potential dependence (z : distance to the wall). We present detailed results of two series of experiments at a Cs vapor/dielectric window interface on the $6S_{1/2}$-$6P_{3/2}$ (λ = 852 nm) resonance line and on the $6S_{1/2}$-7P second resonance line (λ = 455 nm and λ = 459 nm). Lineshape analysis at various pressures consistently shows that a van der Waals-type surface

(*) Laboratoire Aimé Cotton, CNRS II, Bât. 505, Université Paris-Sud, F 91405 Orsay, France.
(**) URA 282 du CNRS.

attraction has to be considered to interpret strong lineshape distortions and resonance shift. The attractive strengths are found to be equal respectively to ≈ 2 kHz μm^3 and ≈ 20 kHz μm^3, independently of the considered hyperfine component, within the experimental accuracy. It yields also typical parameters of pressure broadening and shift, which are shown to originate in collisional processes, at densities where the medium is opaque. Theoretical expectations for the VW strength are discussed on the basis of the results of atomic theory. The predicted values are smaller, by a typical factor of 2, than those deduced from the experiments. The validity of the theory, when applied to a dielectric interface, is discussed and seems questionable when the frequency of virtual atomic transitions involved in the van der Waals attraction potential lies in the dielectric window absorption range.

1. Introduction.

In its principle, reflection spectroscopy at an interface with a vapor is a convenient tool for exploring atom-surface interaction. Recently, a systematic frequency-shift between Doppler-free (volume) saturated absorption (SA) resonances and normal incidence frequency-modulated (FM) selective reflection (SR) signals has been demonstrated in various experiments performed at the boundary between a dielectric and alkali-vapors (by our group with Cs, on the D_2 resonance line $\lambda = 852$ nm [1] and on the second resonance line $6S_{1/2}$-$7P_{1/2, 3/2}$ [2] $\lambda = 459$ nm, 455 nm ; in Akul'shin's work, with Rb, on the D_1 line $\lambda = 794$ nm [3]). In our work, we have proved experimentally that the observed shift originated in the surface interaction. Moreover, by comparison with a general theory of (FM) SR for atoms in a potential [4], we have demonstrated that frequency shift as well as the observed lineshape distortions could be entirely described by a z^{-3} interaction potential (z : atom-wall distance). Such a z^{-3} potential was attributed to a London van der Waals term, as it was consistently demonstrated by studying the variations of the SR lineshapes with respect to collisional broadening. These first spectral observations of the VW surface attraction made possible the measurement of the VW attraction exerted on short lifetime atomic state, to which no access was provided by the few experiments demonstrating VW surface attraction through mechanical deflection of an atomic beam [5-7].

The aim of the present paper is to get a deeper insight both experimentally and theoretically on the atomic parameters controlling the strength of the van der Waals (VW) interaction, as observed in a SR experiment. The paper is presented as follows : in a first part (Sect. 2), we describe the various natures of the surface interaction which can be involved for atoms flying close to a surface. In the following section (Sect. 3), we recall the main results of the theory of (FM) SR for atoms moving in an inhomogeneous potential and we present the corresponding results for various types of potential (including an overall repulsive VW potential). Next section (Sect. 4) is devoted to a description of the experimental set-up and is followed by a detailed analysis of the experimental results for all the explored hyperfine components (Sect. 5). In the last part (Sect. 6), we discuss the predictions of the atomic theory for the VW strength along with the influence of the optical properties of the dielectric window.

2. Atom-surface interaction.

2.1 SHORT RANGE AND LONG RANGE INTERACTION. — The strongest interactions between an atom and a surface are always short-range interactions i.e. when the distance is typically comparable with atomic sizes. This short range part of the interaction, which always ends up by a repulsive bareer at very short distances, describes as well chemisorption and physisorption mechanisms. In general, the involved interaction energy exceeds by several orders of magnitude the width of optical transitions for free atoms. Energy eigenstates to be

considered are no more related with a free atom, but are the one of some adatom, strongly depending on the surface structure. This means that high resolution spectroscopy is not necessarily of a great help ; and although the interaction can seem quite strong, it provides a negligible contribution (some eventual ultra broadband resonant background) in SR technique, as the typically probed region extends as far as $z \approx \lambda_{\text{laser}}$.

On the other hand, a « free-atom » in the neighborhood of some surface interacts with it because the presence of the surface alters the boundary conditions for the unavoidable interaction between the atom and the e.m. vacuum. This atomic sensitivity to the environment typically extends to an optical wavelength. This implies that, provided that the strength of these interactions is not too weak, significant deviations are to be expected between SR spectroscopy and bulk spectroscopy of the same atomic species. One expects also a much smaller influence of the very nature of the surface than in the case of short range adsorption mechanisms. Although quantum electrodynamics theory (cavity QED) provides a unified view of the atom-boundary interaction [8], involving both atomic energy renormalization and modified properties for the spontaneous emission, it can be useful to divide the resulting interaction in the three following regimes : (i) London-van der Waals regime, (ii) Casimir Polder contribution, (iii) spatially varying properties of the spontaneous emission due to the boundary-perturbed vacuum fluctuations (resonant interaction).

2.2 THE LONDON-VAN DER WAALS ENERGY SHIFT. — From an electrostatic point of view, an electric dipole d, in the vicinity of a perfectly conducting plane, induces a symmetric dipolar image, which attracts the object dipole with a potential energy V_{VW} governed by :

$$V_{\text{VW}} = -\ (d^2 + d_z^2)/16\, z^3 \tag{1}$$

where d_z is the dipole component normal to the metal boundary ([1]).

If the metal is replaced by a dielectric boundary, the induced image is smaller than the object dipole by a factor $(\varepsilon - 1)/(\varepsilon + 1)$, where ε is the electric permittivity of the dielectric medium.

The quantum-mechanical analog of this classical approach is straightforwardly obtained by replacing in equation (1) d by the dipole operator D of the atomic system. A neutral atom, lying in the vicinity of a surface, can be viewed as a fluctuating dipole, resulting in non zero attraction by its correlated image [i.e. $\langle D^2(t)\rangle \neq 0$, although its time-averaged value vanishes, $\langle D(t)\rangle = 0$]. These dipolar fluctuations are described by the quantum-mechanical expectation value of the $D^2 + D_z^2$ operators.

For an atom in the eigenstate $|i\rangle$, one has :

$$\langle i\,|D^2 + D_z^2|\,i\rangle = \sum_j \left\{ |\langle i\,|D|\,j\rangle|^2 + |\langle i\,|D_z|\,j\rangle|^2 \right\}. \tag{2}$$

In equation (2) the summation over j extends to all levels coupled to the $|i\rangle$ state by virtual dipole transitions, and the reduced matrix element D_{ij} is simply related to i-j atomic transition probability by (in a *scalar* approach) :

$$|D_{ij}|^2 = \frac{3}{4}\hbar\gamma_{ij}\left(\frac{\lambda_{ij}}{2\pi}\right)^3 \tag{3}$$

If such a treatment is rather usual, difficulties arise when the boundary is a dielectric material instead of a perfect conducting plane, especially when it is a dispersive medium [i.e.

([1]) One assumes $4\pi\varepsilon_0 = 1$.

$\varepsilon = \varepsilon(\omega)$]. However, for a purely transparent dielectric (ε real), the VW attraction should write :

$$\langle V_{\mathrm{VW}} \rangle_i = -\frac{1}{16\, z^3} \sum_j \frac{\varepsilon(\omega_{ij}) - 1}{\varepsilon(\omega_{ij}) + 1} \left(|D_{ij}|^2 + |D_{z,ij}|^2 \right). \tag{4}$$

In all cases, this attractive potential leads to a red energy shift. For excited levels, the above self reaction to atomic fluctuations also leads to modified rates of spontaneous emission : as it is well known, total inhibition of the emission rate (or doubling, depending on the considered polarisation) can occur in the close vicinity of a reflecting boundary [9]. These points will be discussed in section 2.4. Let us notice however at this step that these last effects are strongly attenuated in the neighborhood of a dielectric medium.

2.3 CASIMIR AND POLDER INTERACTION. — Instantaneous reaction between a dipole and its image is only a nonrelativistic approximation. Casimir and Polder have shown [10] that when one includes retardation effects in the London-van der Waals dipole interaction, the attraction varies like $z^{-3} f(z)$ where $f(0) = 1$ and $f(z)$ decreases monotonically with z with an asymptotic behavior in $\mathcal{C}/z$ for $z \to \infty$. ($\mathcal{C}$ being a constant depending on the atomic system). Retardation effects become important when $z > \lambda_{ij}$, so that the z^{-4} coefficient for the asymptotic surface attraction is hence related with atomic static polarizability α_x, α_y, α_z. One finally gets the Casimir-Polder contribution for $z \gg \lambda$:

$$\langle V_{\mathrm{CP}} \rangle = -\frac{\hbar c}{8\, \pi z^4} (\alpha_x + \alpha_y + \alpha_z). \tag{5}$$

It should be noticed that due to these retardation effects, the surface attraction decreases relatively to the London-van der Waals predictions and differences with the latter ones should be notable only when the surface interaction has dropped down to very low values. This shows the great difficulty for observing the Casimir-Polder effect, and this explains that, until now, only very few experimental demonstrations of the Casimir-Polder effect have been proposed [11]. An extra-difficulty is related with the fact that much stronger surface interactions are exerted on excited atoms. Indeed, oscillating terms associated to spontaneous emission make the z^{-4} contribution negligible.

2.4 SPATIAL OSCILLATIONS IN RESONANT INTERACTION WITH VACUUM FLUCTUATIONS. — Enhancement or inhibition of spontaneous emission inside a cavity (or near a wall) has become a standard evidence for boundary effects in QED. Indeed, changes in the mode structure of the vacuum field modify the spontaneous emission diagram : for a simple picture, one has to consider interferences between the field spontaneously emitted by the atom, and the reflection of this same field. This leads naturally to spatial oscillations of the spontaneous emission characteristics normally to the boundary, with a (pseudo-) periodicity related to λ_{eg} where λ_{eg} is the wavelength of the considered radiative transition. These (damped) spatial oscillations of the relaxation rate come with analogous oscillations in the transition frequency.

An extensive treatment in the case of a two-level atom have been made by various authors [8, 12]. In [8], an attempt is made to separate « self reaction » contributions (related to atomic fluctuations) and « vacuum fluctuations » contributions. The van der Waals term and the Casimir-Polder term then appear as having different origin (self reaction *vs.* vacuum fluctuations) and are respectively associated with a physical interpretation of two different asymptotic limits $z \to 0$, and $z \to \infty$) of a single QED approach. This approach unifies

electrostatic contributions (related with virtual transitions) and resonant contributions (typical of spontaneous emission for excited levels). It also yields the spatial dependence of atomic relaxation whatever the distance to the wall may be. On the other hand, an important restriction of such a two-level approach is that a two-level model cannot deal efficiently with virtual transitions. Indeed, in the absence of dipolar coupling with at least an extra third level, the VW shift ($z \to 0$ limit) is exactly identical for the ground and the excited states, so that, strictly speaking, a two-level model is not able to predict a spectral shift of a resonance transition for $z \to 0$.

However from this two-level model, we learn that, for each individual level, the amplitude of the VW energy shift (for $z < \lambda/10$) is much larger than the oscillating resonant contribution to the energy shift. Moreover, although extrapolation to a dielectric boundary of the full QED treatment seems to remain an open question, it should be expected that spatial variations of the relaxation rate are considerably damped when the boundary is only a partially reflecting surface (i.e. case of a dielectric).

As one will see below, SR spectroscopy signal is the result of a spatial averaging. Hence, in the following, we will essentially concentrate on the VW red-shift contribution (i.e. $z \to 0$) for a multi-level atom, while neglecting spatial oscillations of the relaxation rate.

3. Selective reflection spectroscopy of interacting atoms.

3.1 PRINCIPLE OF SR SPECTROSCOPY. — Let us first recall that SR spectroscopy [13] consists of monitoring the reflectivity change $\Delta R(\omega - \omega_0)$ at an interface when the illumination frequency is scanned through an optical resonance of medium 2 (see Fig. 1). For homogeneous media and in the framework of a *local* response theory, the reflectivity is simply predicted by Fresnel formulae :

$$R(\omega - \omega_0) = \left| \frac{n_1 - n_2(\omega - \omega_0)}{n_1 + n_2(\omega - \omega_0)} \right|^2 \tag{6}$$

where n_1 and n_2 are respectively the complex indices of medium 1 and 2. (For conveniency, especially when atomic velocity distribution will have to be considered, we restrict ourselves to normal incidence).

If n_1 is purely real (i.e. medium 1 is transparent), and for weak optical densities in medium 2 (i.e. $|\Delta n_2(\omega - \omega_0)| \ll n_2$), the SR signal is, at first order, only sensitive to the dispersive contribution of the resonance Re $[\Delta n_2(\omega - \omega_0)]$. A notable interest of such a reflection spectroscopy is that the atomic response of medium 2 essentially originates in a region located in the vicinity of the interface (within one wavelength).

For a more general understanding of the principle of SR spectroscopy, one has to take into account the spatial inhomogeneity of the atomic response (spatial dispersion) and to consider

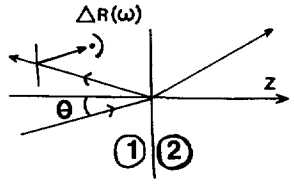

Fig. 1. — Principle of selective reflection spectroscopy. The medium is a resonant vapor, medium 1 is a dielectric window. Incidence is normal ($\theta = 0$) in most of our experiments.

the overall interference of all the fields radiated by resonantly induced microscopic dipoles [14, 15]. Assuming a monochromatic irradiation, and a low optical density in medium 2 (so that absorption is negligible over one wavelength), one calculates at $z = 0$, the resonantly radiated field amplitude $\Delta\mathcal{E}_r$ ($\Delta R \propto \mathrm{Re}\,\Delta\mathcal{E}_r$) :

$$\Delta\mathcal{E}_r = \frac{ik}{(n_1 + 1)} \int_0^{+\infty} p(z) \exp(2\,ikz)\,dz \tag{7}$$

$p(z)$ being the amplitude of the induced atomic dipole at z. The oscillating phase factor $\exp(2\,ikz)$ appearing in equation (7), is related with round-trip light propagation between the wall and the atom. It is responsible for the spatial resolution of the SR method, which is essentially of the order of λ (or $\lambda/2\,\pi$). Indeed, if it can seem at first sight that the whole half-space integration is required for calculating the SR signal in the simple case $p(z) = p_0$, the important point is that slow z-variations of $p(z)$ can be ignored in evaluating the SR signal. As atomic response discontinuity is expected only at the surface, one realizes that only rapid variations of $p(z)$ at a typical distance $z \leqslant \lambda$ will be monitored through SR spectroscopy technique [16]. Another point to be noticed is that, if the signal is proportional to $\mathrm{Re}\,p$ (i.e. dispersion) for a *homogeneous* medium, it results actually from a mixture of absorption and dispersion ($\mathrm{Im}\,p(z)$ and $\mathrm{Re}\,p(z)$ respectively).

If such a way of revisiting Fresnel formulae can seem rather trivial, it is however important to point out that peculiar spatial distribution of atoms can result in providing an absorption signal instead of a dispersive one. Indeed, the surface interaction generates quickly varying spatial inhomogeneities, and this will result in an intricate mixing of resonant absorption and dispersion.

3.2 ATOMIC MOTION AND SELECTIVE REFLECTION. — When SR spectroscopy is performed at the interface of a vapor of moving atoms, the induced microscopic dipole $p(z)$ depends nonlocally on the incident field (i.e. $p(z)$ depends on $E(z')$ with $z \neq z'$) [14, 15].

However, if moving atoms have reached a permanent regime of interaction with the field, one solely expects a Doppler-broadening of the response relatively to the one calculated for motionless atoms. This is how the classical theory of SR spectroscopy at a vapor interface, as developed by Wood [13], predicts the observation of a dispersive Voigt profile. Actually, atomic collision with the surface generally destroys the optical excitation of arriving atoms. In particular, this seems unavoidable when either adsorption mechanisms trap the atom for a while (i.e. in the absence of special surface coatings), or the short-range surface potential is sufficiently diverging that the optical dipole phase is randomized in the surface collision. This implies that departing atoms (if any), follow a transient evolution in their interaction with the field, while the velocity-integration over arriving atoms (in a permanent regime) is limited to half-space $v_z < 0$.

This discontinuity in the velocity integration is responsible for an extra symmetric sub-Doppler contribution in the SR response, which is currently observed in experiments [17]. Moreover, with the additional trick of an applied FM to the incident field, and coherent detection of the induced modulated reflectivity change, the signal becomes the derivative of the initial SR lineshape. Hence, in the large Doppler approximation, the only observable signal is the derivative of the extra-sub-Doppler contribution, which turns out to be purely Doppler-free and antisymmetric [18].

Singling out this narrow contribution presents two essential interests : (i) it provides one of the very few methods of linear spectroscopy which is both Doppler-free and applicable to a cell ; (ii) the contribution essentially originates in atoms with slow normal velocity

($v_z \approx 0$), so that the observed atoms remain close to the surface (within λ) during all of their lifetime and can sensitively experience long-range surface interaction.

3.3 PREDICTIONS OF THE (FM) SR THEORY IN THE PRESENCE OF A z^{-3} VW POTENTIAL. — In [4], a general theory of SR has been presented for the case when the atoms of the vapor move in a potential. In particular, it is shown that various results obtained for SR spectroscopy of potential-free atoms can be generalized. Provided the velocity distributions of incoming and departing atoms are equivalent, the sub-Doppler contribution of these two groups of atoms are identical. Moreover, the use of a FM technique provides a way for isolating a purely Doppler-free contribution ($v_z \approx 0$), particularly sensitive to the surface interaction. Formally, this FM technique allows one to perform directly the velocity integration in the Doppler limit. For a z-dependent potential affecting both energy and transition linewidth, one has :

$$\frac{dR}{d\omega} \propto \mathrm{Im} \int_0^{+\infty} \int_0^{+\infty} dz\, dz' \exp ik\,(z + z')\, \frac{z - z'}{\mathfrak{L}_0(z) - \mathfrak{L}_0(z')} \tag{8}$$

where $\mathfrak{L}_0$ is defined by :

$$\frac{d\mathfrak{L}_0}{dz} = \frac{1}{2}\,\gamma(z) + i\,[\omega_0(z) - \omega\,]\,. \tag{9}$$

Applications to a VW-type potential, which changes the resonance frequency according to :

$$\omega_0(z) = \omega_0 - \frac{C}{z^3} \tag{10}$$

while the dipole decay rate $\gamma/2$ remains constant, were also considered in that work, and are the basis for the interpretation of the experimental results presented in the following sections. We briefly recall here the most striking results of the calculations performed for this type of potential.

A single dimensionless parameter A, defined as :

$$A = 2\,C k^3/\gamma \tag{11}$$

governs the predicted VW shifted lineshape. Computer calculations are easily performed for a (FM) SR experiment since in the double integration (over space, as in (7) and over the temporal — or local — evolution of each individual dipole, while the velocity integration is already eliminated by the use of FM technique), one of the space integration can be performed by purely analytical means. In previous papers only the case of an overall attractive VW interaction ($A > 0$) was considered : indeed if VW attraction red-shifts the energy level of both ground and excited states, one expects a larger shift (due to higher atomic polarizability) for the excited state and hence a red-shift of the transition energy (see the discussion in Sect. 6). Formally, the case of a blue VW shift (i.e. $A < 0$) can be considered as well, and the corresponding results are also presented here (see Fig. 2).

In the weak attractive VW regime ($0 < A \ll 1$), one notes that the (FM) SR lineshape is (more or less) slightly distorted relatively to the ideal antisymmetric lineshape predicted for $A = 0$, while its zero is red shifted. Also the red wing appears broader than the blue one. Surprisingly enough, and as suggested by Alekseev [19] for a blue VW shift of the transition energy ($A < 0$, $|A| \ll 1$), the predictions are very much similar to $A > 0$, except maybe for the far wings behavior and the overall amplitude. In fact, and as already noticed in subsection 3.1, the integration over the spatially inhomogeneous shift mixes dispersion and absorption (or gain). This evidences how blue-shifted complex resonances can algebraically

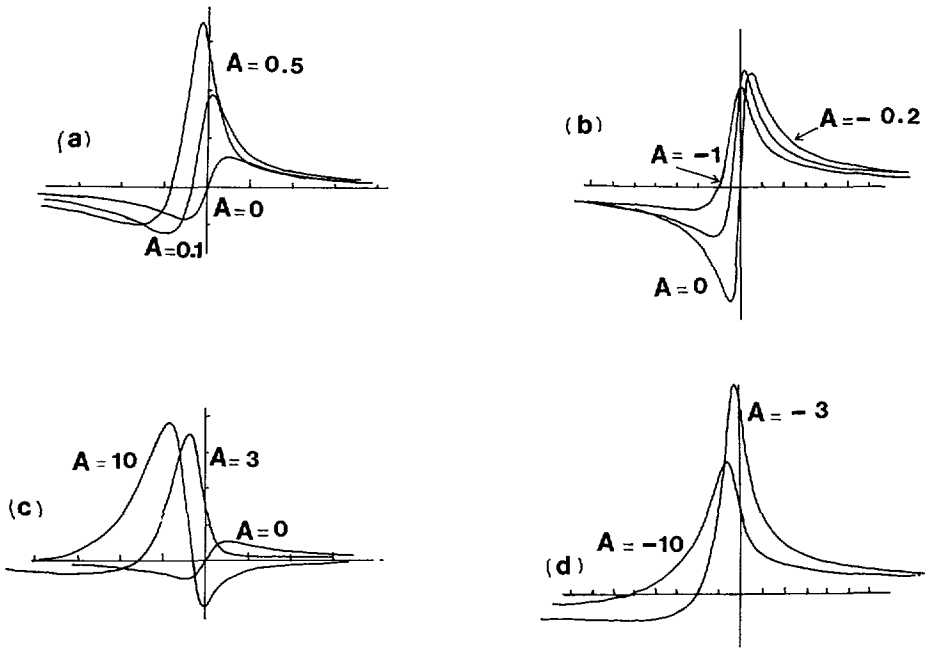

Fig. 2. — Theoretical predictions for (FM) SR lineshapes in the presence of a VW potential under various regimes : (a) weak VW attraction, (b) weak VW repulsion, (c) strong VW attraction, (d) strong VW repulsion (vertical scale is 8 times the one of (b)).

sum up and result in an apparent red-shift (see also appendix A, in which this point is compared with the overall blue shift resulting from absorption along the propagation of incident beam). In the strong VW regime ($|A| > 1$), there is a persistent red-shift of the VW distorted lineshape whatever the sign of the VW interaction is. However, notable differences appear in the quite anomalous lineshapes which are so predicted. In particular, the inverted (and shifted) quasi dispersive lineshape (for $A \approx + 10$) seems quite typical of an overall red-shift, and no negative values of A produce an equivalent lineshape.

3.4 THEORETICAL PREDICTIONS FOR OTHER TYPES OF POTENTIAL. — On the basis of the general theory (Eq. (8)) calculations can be performed for various types of potential. In particular, in the spirit of reference [6], we have evaluated the prediction for $- C_2/z^2$ and $- C_4/z^4$ potentials (see Figs. 3 and 4) which are close to VW potential. However mathematical

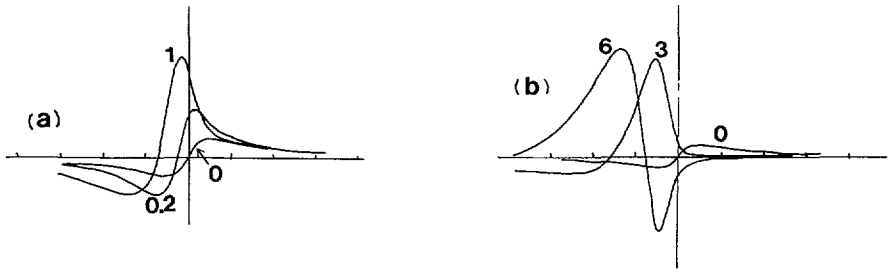

Fig. 3. — Theoretical predictions for (FM) SR lineshapes in the presence of an attractive $- C_2 z^{-2}$ potential, with $A_2 = 2 C_2 k^2/\gamma$ as indicated (a) weak attraction, (b) strong attraction.

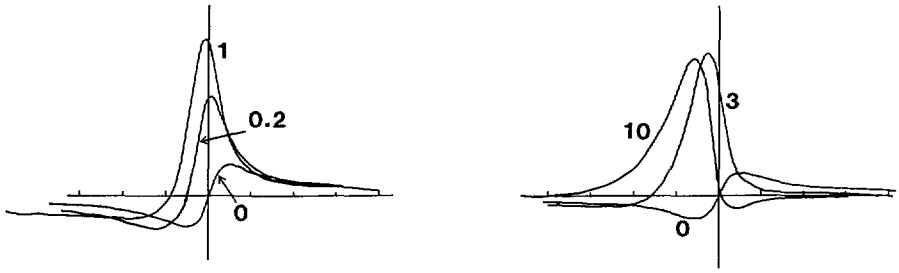

Fig. 4. — Same as figure 3 for a $-C_4 z^{-4}$ potential, with $A_4 = 2 C_4 k^4/\gamma$ as indicated.

difficulties arise in applying Equation (8) to more elaborate potentials. In particular, the long range resonant surface potential considered in subsection 2.4 is both spatially oscillating and with coefficients defined by special functions. Hence, one can expect that atomic motion will tend to wash out oscillating potentials much more than monotonic ones.

4. Experimental set-ups.

4.1 PRINCIPLE : COMPARISON WITH SATURATED ABSORPTION. — Until now, our work has essentially dealt with two series of systematic experimental studies, one on the D_2 resonance line $6S_{1/2}$-$6P_{3/2}$ of Cs vapor ($\lambda = 852$ nm), the other one, on the second resonance line $6S_{1/2}$-$7P_{3/2}$ ($\lambda = 455$ nm) or $6S_{1/2}$-$7P_{1/2}$ ($\lambda = 459$ nm) of Cs. In both cases, we have essentially investigated the (FM) SR frequency lineshapes at a glass or sapphire interface with Cs vapor. Most of the efforts were devoted to the observation of SR spectra in nearly ideal conditions, as close as possible to the theoretical model, implying : *normal incidence*, suppression of power and pressure broadenings, . . As this is finally obtained at the expense of the signal-to-noise ratio, experiments in slightly different conditions were also conducted for purposes of extrapolation. A systematic study of pressure effects (self-broadening or shift) was also worth being done because SR spectroscopy is a quite convenient tool for probing optically dense vapors. To get a frequency reference (absolute frequency marker and control of the laser frequency scan) a peripheral saturated absorption (SA) experiment on an auxiliary Cs cell is always performed simultaneously with the SR experiment. For this SA experiment, great care is taken in eliminating all possible causes of frequency shift or broadening (low Cs pressure, low incident intensities, reduced laser jitter) or lineshape distortion. In this view, and although a FM is already applied to the laser beam for the SR experiment, (FM) SA experiment was often used as a simple preliminary control of the applied FM (symmetry and phase adjustment), and replaced with an amplitude modulation (AM) solely applied to the pump beam in order to eliminate the background due to the probe absorption.

Practically, SA experiments at $\lambda = 852$ nm were performed at room temperature in a 2 cm Cs cell (i.e. pressure 10^{-6} Torr) with pump and probe beams of 5 μw (beam diameter — 2 mm), while in the blue region, the same 2 cm cell is heated up to 60 °C (a few 10^{-5} Torr) and the incident beams have a typical intensity of 100 μW.

4.2 LASERS AND GENERATION OF THE FM. — The laser sources are respectively a diode laser for $\lambda = 852$ nm (output power : ~ 15 mW) and a standing-wave single-mode dye laser with Stilbene 420 for $\lambda = 455$-459 nm (output power < 2 mW). Because the natural width of the excited states are respectively 5 MHz (6P) and 1.3 MHz (7P), there is a crucial need of reducing the laser frequency jitter below a typical 1 MHz value. For the diode laser, this has been achieved by the technique of weak optical feedback coupling *via* an external confocal

Fabry-Perot (FP) cavity while the dye laser was commercially provided with active locking on an external FP. In both cases, laser frequency scans are produced *via* scanning the external Fabry-Perot length. To produce the frequency modulation, an extra sine-wave modulation was applied to the FP length in each case.

For the diode laser, the FP length was controlled through a PZT. To prevent an induced asymmetry related with hysteresis, two separate PZTs were used, a long (and slow) one for the frequency scan, and a short one for the FM permitting a modulation at a typical value of 37 kHz ; although at such a high frequency the servoloop controlling the diode FP distance is totally blind, this makes no trouble to the laser locking mechanism because the frequency excursion remains quite modest, typically below 2 MHz.

For the commercial dye laser the length of the temperature-stabilized sealed FP was controlled through a galvo-mounted plate. Hence, the frequency of the modulation, typically set at 630 Hz in our experiments was nearly at its maximum. A notable inconvenient of this low-frequency FM is that the technical amplitude noise of a dye laser is quite important in this range. Moreover, the locking system for the dye laser frequency follows only hardly the relatively fast FM applied to the FP. This generally results in some added (coherent) amplitude noise to the dye laser output. Hence, for sensitivity purposes, it was necessary to insert an intensity-stabilization system at the output of the laser. Since a higher FM frequency could have seemed desirable, and also because the peripheral SA experiment does not intrinsically require a FM laser, we also tried to generate the FM externally to the laser. Unfortunately, the generation of a clean FM sine wave requires one to use the (EOM or AOM) modulators in a low-transmission regime, so that the typical available power drops much below 100 μW. In such a range of power, the reflected intensity R itself becomes quite low (< 1 μW) so that the electronic noise of the detection (NEP of the photodiode and amplifiers is a few 10^{-11} W/ $\sqrt{\text{Hz}}$) would make it difficult to observe small variations ΔR of the reflectivity.

4.3 VAPOR CELLS. — Several sealed Cs cells were used for these SR experiments. In all cases, these cells had to be heated up (in the range 90-200 °C for $\lambda = 852$ nm, in the range 170-260 °C for experiments in the blue region). For this purpose, the Cs cells are inserted in a system of two metal boxes, one containing the body of the cell, the other one the Cs reservoir. Each box is independently heated up by electric wire, and isolated by glass wool. Hence two temperature regions are defined and this permits overheating of the windows relatively to the Cs reservoir. Inside the metal box containing the body of the cell, two holes are drilled for incoming light to penetrate into the cell through the oven system. An extra pair of glass windows is located in front of the holes in order to reduce thermal flux. Similarly, a small hole is drilled in the oven for Cs reservoir, in order to get approximately equivalent thermal dissipation for both regions. For one of the cells whose whole body was in copper, a radiator was placed between the two boxes in order to generate some kind of isolation between these two regions in spite of their strong thermal coupling.

Temperatures in each box were monitored with a thermocouple and care was taken to maintain a temperature difference between the two boxes not exceeding 10 °C. This is to reduce the effect of a possible gradient between the temperature measured in the lower box, and the effective vapor temperature. Hence Cs vapor pressure was estimated from Langmuir-Taylor formulae. The absolute uncertainty on the pressure scale was estimed not to exceed 40 % (corresponding to an uncertainty of ~ 3 °C in the absolute temperature measurement), although relative pressure variations inside a series of measurements are measured with a much better sensitivity (~ 10 %, < 1 °C).

The essential difference between the various cells lies in the nature of their windows (glass or sapphire). At least three types of cell were used :

i) glass cells, with pyrex or quartz windows ;

ii) a copper-cell with (birefringent) sapphire windows, ended either by a Cs glass reservoir (for low temperature experiments i.e. $\lambda = 852$ nm), either by a Cs copper reservoir (experiments in the blue region require higher temperatures, at which Cs vapor chemically attacks glass-metal transitions and generates leaks) ;

iii) a glass cell, — same as i) type — in which a polished sapphire plate was inserted and layed down on the original glass window, the body of the cell being installed vertically. Such a cell was used only in a few experiments (at $\lambda = 455$ nm), but corresponds to a promising design for a simultaneous comparison between a glass interface (on the top) and any other special interface (on the bottom) : indeed, it guarantees that the two simultaneous experiments are performed with the same vapor interface (independently of the temperature readings, or of the pressure estimates) and it does not require the technologically difficult sealing of a special window to the cell body.

The faces of the windows are essentially parallel. Ideally, they should have been designed with a wedge sufficient to eliminate interference effects between the inner and the outer faces of the window. Actually, their thickness ($<$ a few mm) is small enough so that in the frequency range (< 1 GHz) explored across atomic resonances, no sensitive changes of the windows reflectivity occur due to interferometric effects.

A more essential problem is the very nature of the surface window. Although the cells are first evacuated to $< 10^{-7}$ torr before being filled with Cs, no special attention could be paid to avoid surface contamination. In fact, the possibility of contamination by the vapor itself is intrinsic to the principle of a sealed cell. Moreover, it even happened several times in the temperature cycling process that the windows get accidentally colder than the reservoir : a Cs deposit appears on the windows, removable only after reinverting the temperatures. Once the windows have returned to their normal transparency (as can be checked through their off-resonance reflectivity), no significant differences in SR lineshapes could be observed between recordings taken before or after this temporary coverage of the window. Of course, this cannot rule out the quite realistic hypothesis of a permanent thin layer on the window. However, it seems reasonable to expect that when probing long-range surface interaction, the « bulk » properties of the window (at least within λ) are more important than the detailed nature of the first atomic layers at the interface. As we shall see below (Sects. 5 to 7) such an expectation seems confirmed by observed differences between glass and sapphire interfaces.

4.4 Optical set-up.

4.4.1 *Polarization.* — The optical set-up for the (FM) SR experiment is quite simple, both in its principle and its realization. Most of the experiments are performed at normal incidence. The reflected beam has then to be picked-up with a beam splitter, or can be ejected by a Glan prism polarizing beam splitter if a $\lambda/4$ plate (or another polarization rotating system) is inserted between the Glan prism and the Cs cell. Both techniques were currently used. If the last one enables us to pick-up all of the reflected beam, this is important only when the sensitivity (for this linear spectroscopy experiment) is limited by the too low laser intensity relatively to the background detection noise. Anyhow, playing with polarization for detection purposes is possible only if no other effects related with polarization are to be expected. Optical pumping which requires ultra low incident intensity to depopulate a hyperfine level should be sensitive to the incident polarization, especially on the first resonance line. One could notably expect a polarization dependent absorption length in the vapor, which could influence the SR signal. Actually, no differences between linearly and circulary polarized light even on the $F = 4 \rightarrow F' = 5$ transition (which is possibly free of population transfer through

optical pumping) could be noted in preliminary experiments. Hence, the incident polarization was chosen only according to experimental conveniency.

4.4.2 *Incidence angle.* — Typical accuracy for the « normal incidence » was of the order of 1 mrd, and was essentially limited by the incident beam natural divergence. An investigation of incidence angle has been carried out, in a range limited to < 100-150 mrad because of geometrical limitation related with the system of double windows. We observed the residual Doppler broadening predicted by the theory [15, 20], as well as the predicted reduction of SR lineshape distortions induced by surface interaction [4]. However, it is beyond the scope of this paper to report in detail on these experiments, as it did not bring until now new informations on the VW interaction, but makes its measurement more difficult.

5. Experimental results, and interpretation in the VW attraction model.

5.1 FITTING A SR SPECTRUM WITH THEORY. — The beauty (or difficulty) of VW potential applied to SR theory lies in the fact that a single parameter (A in reduced coordinates) governs simultaneously the frequency-shift and severe lineshape distortions, which even lead to quite anomalous lineshapes in the strong VW regime. For effectively fitting a given experimental SR lineshapes, two extra parameters have to be adjusted, namely the frequency scale and the amplitude scale. In most cases, the amplitude of the measured (FM) SR signals is somehow arbitrary, because it necessarily depends on the atomic density, on the FM amplitude, on possible aperturing effects of the detected optical beam, etc.. As far as frequency scale is concerned, the normalized width γ is always meaningful and related with the various broadening mechanisms suffered by the medium. Hence, consistency is expected in the variations of the widths — as determined by the fits — when a series of experimental results is analyzed. The strength of the potential, which is in many cases the most significant physical quantity, and which should be in most cases independent of the details of the experimental conditions, is determined by the $A\gamma/2$ product.

Practically, the fitting procedure, which involves three adjustable parameters, is divided in two iterative steps, one consisting of adjusting the scale parameters for a given (guessed) A value, the other one is related with exploring different acceptable A values chosen in a catalog of tabulated A values. Indeed, the limited signal-to-noise ratio sets the required accuracy for the A value (of the order of 5-10 % in the most favorable case of a strong VW regime, i.e. for $A > 1$) so that there is no need to perform each time the computation of a (more or less) converging series of A curves.

Although a least square-fit procedure can determine the scale parameters for a given A value, a manual adjustment leads to similar values for the same considerations of signal-to-noise ratio. Moreover, and especially for the weakest hyperfine components, the wings of the SR resonance cannot be always considered as isolated, so that systematic deviations with the fitting lineshapes can be observed. This notably occurs in the presence of pressure broadening. Anyhow, the main point is that some experimental SR resonances can be fitted with VW potential SR lineshape (and accuracy of the fitting parameters is hence easily evaluated), while some others can not. This typically occurs when the metallic vapor is sticking on the window (so that even in the absence of surface interaction, the SR lineshape is no longer predicted to be antisymmetric) and, up to some extent, when the irradiating beam is saturating.

5.2 EXPERIMENTAL RESULTS.

5.2.1 $6S_{1/2}$-$7P_{3/2}$ ($\lambda = 455$ nm). — The most complete series of measurements was carried out on the $6S_{1/2}$-$7P_{3/2}$ ($\lambda = 455$ nm) transition. Table I presents the results of a systematic

Table I. — *Experimental values for the various hyperfine components of the* $6S_{1/2}$-$7P_{3/2}$ *line, as resulting from the pressure analysis. Estimated uncertainties (in parentheses) result both from uncertainty in extrapolating the typical* VW *parameter from each individual experimental curves, and in the fluctuations with pressure of these parameters (see Fig.* 5*). The uncertainty in the pressure (or temperature) scale is not considered.* $\gamma A/2$ *is the strength of the* VW *potential at* $\lambda/2\,\pi$, Γ *is the slope of the pressure broadening parameter* ($\gamma(P) = \gamma(0) + \Gamma P$ *with* $\gamma(0) = 5.5\ (\pm 0.5)$ MHz *for all hyperfine components), and* Δ *is the pressure shift observed relatively to a purely* VW *shifted* SR *resonance.*

$F \rightarrow F'$	$\gamma A/2$ (MHz)	Γ (MHz/torr)	Δ/P (MHz/torr)
$3 \rightarrow 2$	58(± 6)	110(± 10)	− 35(± 10)
$3 \rightarrow 3$	57(± 8)	110(± 10)	− 45(± 10)
$3 \rightarrow 4$	62(± 8)	125(± 20)	− 50(± 15)
$4 \rightarrow 3$	58(± 8)	130(± 30)	− 40(?)
$4 \rightarrow 4$	57(± 10)	115(± 10)	− 45(± 5)
$4 \rightarrow 5$	52(± 6)	125(± 15)	− 50(± 5)

pressure study on this transition for the 6 hyperfine components, performed under a non saturating irradiation of ~ 25 μW (beam diameter ~ 2 mm). With a recording duration of a few minutes for each component, the experimental sensitivity permits very good fits, with a typical accuracy on adjustment parameters dropping below 10 % in the best cases (notably for the strong 4-5 component). As previously noted [2], in the high pressure range, better fits are provided when accounting for possible additional pressure shift of the resonance : this pressure shift is simply deduced from the comparison with the SA reference spectrum, while the procedure for fitting the SR experimental lineshape with three adjustment parameters remains unchanged.

Figure 5 shows, for each hyperfine component and as a function of pressure P, the experimental value of the normalized width γ, of the strength of the VW potential $A\gamma/2$ and of the frequency shift Δ, as estimated from the best fits. The most striking (and expected) result is that the strength of the VW potential is independent of pressure (for all hyperfine components). This is demonstrated with a 20 % accuracy. In this constant product $A\gamma/2$ the pressure increase of γ (which is responsible for the decrease in A value, and hence for spectacular changes in the SR lineshape) is legitimately interpreted as a pressure broadening, as its variations are linear with pressure ; similarly, the frequency shift appearing in the high pressure range evolves quite linearly with pressure, and should essentially originates in a collisional pressure shift (see appendix A for estimation of the absorption measurement). Extrapolation at zero pressure leads to a γ value ($\approx$ 5 MHz whatever is the hf component) systematically larger than the one predicted from the $7P_{3/2}$ lifetime (predicted optical width of the transition : 1.3 MHz). However, with the blue laser, frequency jitter could never drop below 1 (and sometimes 2) MHz r.m.s., and in the FM, the frequency excursion itself currently reaches 2-3 MHz for sensitivity purposes. As a general result, it

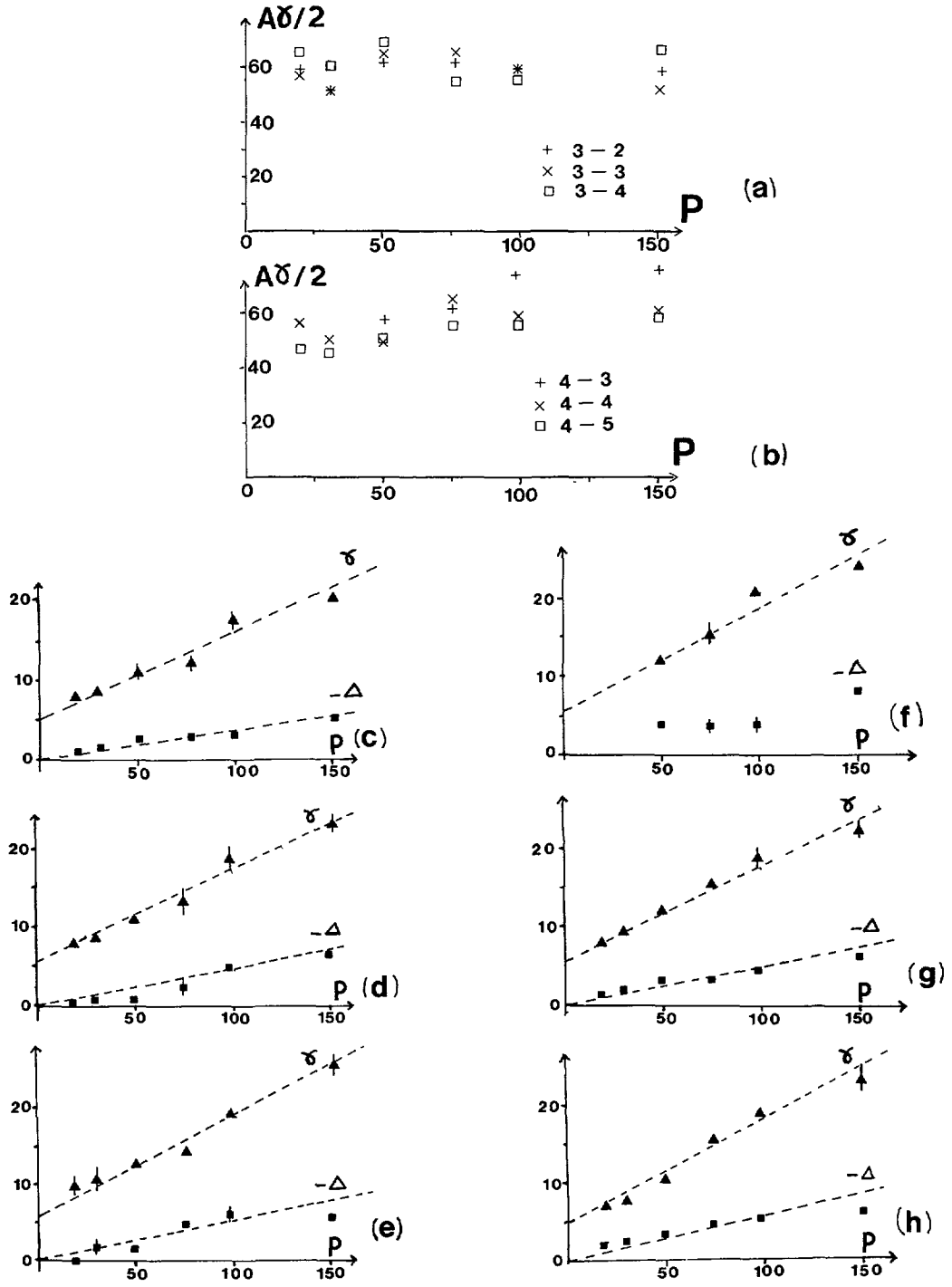

Fig. 5. — Experimental results of the pressure study on the $6S_{1/2}$-$7P_{3/2}$ SR spectrum, as analyzed through SR theory in the presence of a VW potential : (a) and (b) estimated value of the VW attraction at $\lambda/2\ \pi$ for the various hyperfine components ; (c)-(h) estimated width γ(▲) and red-pressure shift-Δ(■) for the respective hyperfine components : (c) 3-2, (d) 3-3, (e) 3-4, (f) 4-3, (g) 4-4, (h) 4-5. Pressure P is in mtorr, VW attraction (at $\lambda/2\ \pi$), width and shift in MHz.

should be noticed that if collisional effects seem to vary quantitatively with the hf component, no significant difference between the VW attraction could be evidenced for the various hf components. The typical VW strength appears to be of the order of 20 kHz μm^3. This will be discussed with more details in the next section, where values of the VW strength will be estimated.

Some types of results, and notably the strong changes in the SR lineshapes related with pressure effects were observed with a quartz cell. A simultaneous comparison between the two interfaces (sapphire/Cs and quartz/Cs) of the two-window-cell (see Subsect. 4.3) was performed at various pressures and always shows stronger lineshape distortions (i.e. stronger VW interaction) for sapphire than for glass. A typical example is provided at figure 6. Both curves can be fitted with a VW (FM) SR lineshape, with respectively $A = 13$ and $A = 9$ [21].

A series of experiments was also conducted for this transition under non normal incidence. Instead of trying to fit the data with an added adjustable parameter (e.g. the residual Doppler width), we present here (Fig. 7) a comparison with an *a priori* theoretical prediction, in which the chosen parameters are the ones determined in the normal incidence series of experiments.

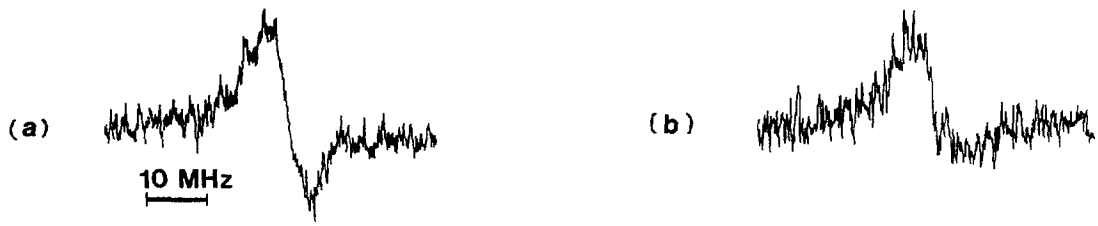

Fig. 6. — Comparison between : (a) a sapphire window and (b) a glass window. Experiment performed on the two-window cell on the $6S_{1/2}(F = 4) \rightarrow 7P_{3/2}(F' = 5)$ transition of Cs vapor ($T \approx 180$ °C).

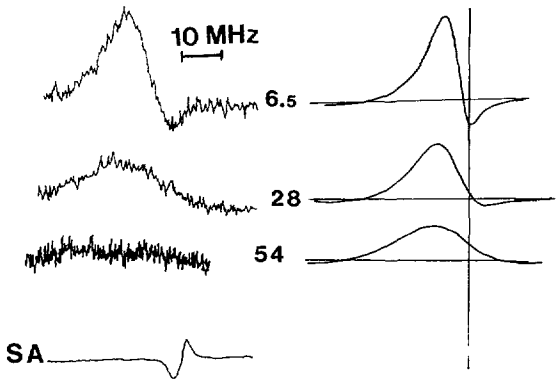

Fig. 7. — Variation of the (FM) SR lineshape with the incidence angle. Comparison between experimental lineshapes (left side) resulting from an experiment performed on the $6S_{1/2}(F = 4) \rightarrow 7P_{3/2}(F' = 5)$ transition for various angles (as indicated, in mrads, at the center) and the corresponding theoretical curves (right side), as predicted with ku $\theta = 450$ MHz, $\gamma = 10$ MHz, $A = 9$, i.e. with the typical parameters describing an experiment under normal incidence at the same pressure (50 mtorr). Relative amplitudes of the theoretical curves are not corrected for experimental increasing aperturing effects. The bottom curve on the experimental side is a (FM) SA spectrum yielding a reference frequency for the transition.

Note that experimental amplitudes are in somewhat arbitrary units, due to various aperturing effects.

5.2.2 $6S_{1/2}$-$7P_{1/2}$ (λ = 459 nm). — As shown in figure 8, analogous distortions of the SR lineshape partly vanishing with Cs pressure-broadening are observed on the $6S_{1/2}$-$7P_{1/2}$ transition and are also to be attributed to the VW surface attraction.

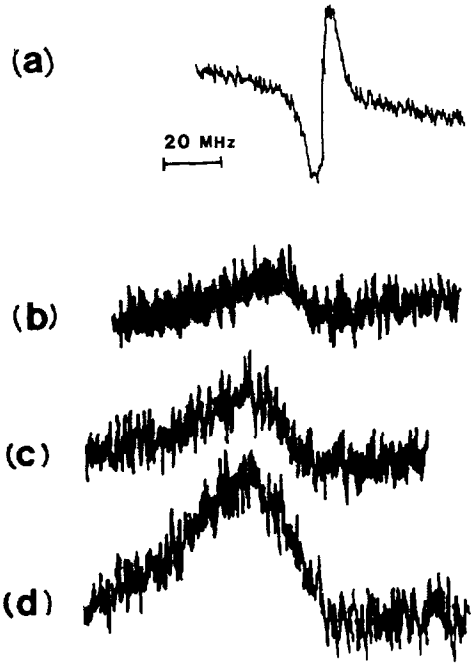

Fig. 8. — (FM) SR spectrum on the $6S_{1/2}(F = 4)$-$7P_{1/2}(F = 3)$ (λ = 459 nm) compared with (a) a reference (FM) SA spectrum, at various Cs pressure : (b) 80 mtorr, (c) 280 mtorr, (d) 335 mtorr. Typical irradiating power is 10 μW.

Unfortunately, the signal-to-noise ratio is much lower than for the $6S_{1/2}$-$7P_{3/2}$ (λ = 455 nm) transition. One of the essential reason for such a situation is related with the emission spectrum of the laser dye, whose lower edge on the red side is ~ 460 nm. It does not mean only that the available power is very weak, but also that one has to deal with an unstable behavior of the laser and frequent mode hoppings. It seems also that transition probabilities for each individual hf component are weaker than for the 455 nm. For all these sensitivity reasons, fitting the experimental curves could be tried only for relatively high pressure, when pressure broadening is already considerable. Satisfactory agreement with theoretical fits can be achieved, but due to the limited sensitivity, it cannot provide a significant measurement of the VW attraction.

5.2.3 $6S_{1/2}$-$6P_{3/2}$ (λ = 852 nm). — The first observation of the surface attraction was performed on this resonance transition. The most striking effect of the surface is the frequency-shift of the SR resonance center relatively to SA resonance center, which in all cases is evaluated to -3 ($\pm$ 1) MHz. Although the SR lineshapes remain quasi-dispersive, they exhibit notable asymmetries, characterized by a broad red wing and a narrower higher

amplitude blue wing. Such a behavior is typical of a weak VW regime, ($A \ll 1$) for which the VW frequency shift at $\lambda/2\ \pi$ remains smaller than the linewidth. Several reasons are responsible for this « weak VW regime », compared to the strong regime observed with the blue transition : the optical width (to which VW strength is compared) is larger while the probed region, typically governed by $\lambda/2\ \pi$, extends farer from the surface ; besides and as it will be discussed later (Sect. 6), the VW potential itself is smaller than for the blue transition.

A large amount of effort was devoted to obtaining SR spectra in conditions in which surface attraction is not partially hidden by strong effects. This was achieved under exact normal incidence, a frequency excursion < 2 MHz for the FM, a laser intensity $< 20\ \mu$W (beam diameter 1-2 mm) and for temperature < 100 °C. Indeed, when these experimental conditions are met, a (reasonable) variation of any parameter is followed by a linear change of the amplitude, while one verifies that the lineshape of the overall spectrum remains unchanged.

In these conditions, at the interface with a sapphire window, experimental SR lineshapes are typically fitted with $A = 0.2$ theoretical lineshapes, without sensitive difference for the various hyperfine components. A typical example of such a fit is provided at figure 9 for the $4 \rightarrow 5$ transition with an effectively measured width ~ 7 MHz (instead of a predicted 5.3 MHz). This leads to a VW attraction of 2 kHz μm^3. If a rather low pressure (0.4 mtorr) is sufficient to observe the SR signal for this resonance transition, one of the difficulty of the experiment is related with strong resonant collisional effects : different techniques had already measured a self-broadening of the transition of the order of 4 GHz/torr [18], while pressure shifts, although never investigated previously, had to be analyzed as they could bias the comparison with low-pressure SA spectra. For these weakly distorted lineshapes, it is convenient to define an experimental shift (VW distortion + extra pressure shift) as the shift of the zero of the signal relatively to the atomic resonance as defined by the saturated absorption experiment. The pressure dependence of this shift is plotted in figure 10. Uncertainties in this pressure shift mostly originate in the considerable pressure broadening of the transition, which can eventually lead to partial overlap of the

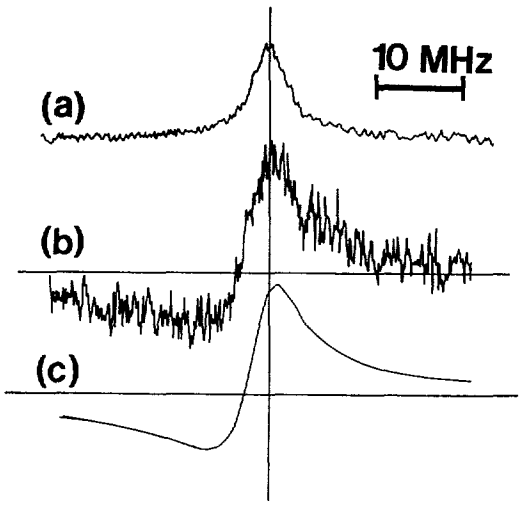

Fig. 9. — Spectral evidence of the VW surface attraction as observed on the $6S_{1/2}(F = 4)$-$6P_{3/2}(F = 5)$ D_2 resonance line : (a) is a reference (AM) SA spectrum ; (b) is the (FM) SR spectrum under a pressure ≈ 0.3 mtorr ; (c) is a theoretical (FM) SR lineshape with $A = 0.2$, which perfectly overlaps the SR spectrum.

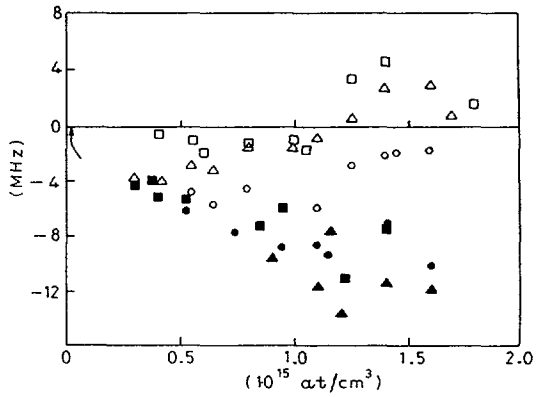

Fig. 10. — Frequency shifts observed on the D_2 line between (FM) SR spectrum and SA (volume) reference spectrum as a function of Cs vapor density. The arrow stands for the typical vapor density at which the analysis of surface interaction is performed. The different types of experimental points correspond to the following hyperfine components : (□) 3-2, (△) 3-3, (○) 3-4, (■) 4-3, (▲) 4-4, (●) 4-5.

various hyperfine components (however these overlaps have negligible influence on the position of the SR linecenters). In spite of the uncertainty, one clearly sees a red pressure-shift for the $F = 4 \rightarrow F' = \{3, 4, 5\}$, and a blue one for the $F = 3 \rightarrow F' = \{2, 3, 4\}$ components. As far as the VW interaction is concerned, the most notable point is that in the typical pressure range of surface interaction observation ($T < 100$ °C), the pressure-shift remains totally negligible, and no extrapolation to low-pressure is required to determine VW strength. As discussed in appendix A, it seems probable that this pressure shift is related with collisional effects, and that blue-shifting optical density effects [14] are negligible.

Similar experiments on this D_2 transition were conducted with glass cells. No significant difference could be observed when comparing with results for a sapphire interface. As the VW attraction is expected to be slightly smaller than for sapphire (one expects A glass $\simeq 2/3\ A$ sapphire, as in subsection 5.2.1), we have to attribute this similar behavior to some lack of accuracy for these experiments in the low VW regime. We have also suspected some contamination of the glass surface, which could explain the slight, but systematic, extra-broadening of the SR resonance.

5.3 FITTING PROCEDURE APPLIED TO VARIOUS TYPES OF POTENTIAL. — As shown above, very demonstrative results are provided by the results on the blue transition which exhibit strong VW distortion. Indeed, independently of the consistency of the series of experiments and fitting curves, it can be seen that other types of potential are not suitable for interpreting results : the experimental signal-to-noise ratio is good enough to evidence significant differences in the overall lineshapes between a VW z^{-3} potential, and neighboring z^{-2} and z^{-4} potentials. In particular, in the strong VW regime, several quantities characterize the lineshape asymmetry : when inverted quasi-dispersive lineshapes are obtained, and even if allowing for an extra-pressure shift relatively to SA linecenter, a signature of the lineshape asymmetry lies both in the ratio of the peak amplitudes and in the ratio of the width of each individual arch. Comparison between $-Cz^{-3}$ (with $A = 10$) and $-C_2 z^{-2}$ potentials (with $A_2 = 6$, A_2 is the strength of the potential in reduced coordinates defined in the same way as in equation (11), i.e. $A_2 = 2\,C_2 k^2/\gamma$) provides (Fig. 11) a simple demonstration of the intrinsic difference between these two lineshapes although they present a similar asymmetry in the amplitude which will be discriminated with sensitive enough experiments. Such a

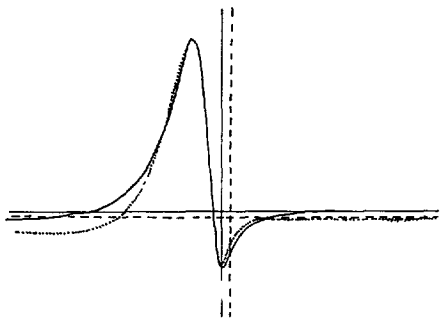

Fig. 11. — Comparison between z^{-3} and z^{-2} types of potential in the strongly attractive regime. Full line corresponds to $A = 10$ (z^{-3} potential). Dotted lines (dashed axes) correspond to $A_2 = 6$ (z^{-2} potential). The scales were adjusted so that the total heights, and the widths at half maximum on the low-frequency broad wing are identical. Note the different base lines implying a different amplitude ratio between positive and negative wings.

discrimination remains possible, although more difficult, when comparing these curves with a $-C_4 z^{-4}$ potential ($A_4 = 20$).

On the other hand, when the surface interaction is weak at the typical observation distance ($< \lambda$) for selective reflection, numerous types of potential can fit a slightly distorted curve. For the typical case of the D_2 resonance line in Cs, several types of long-range potential could fit the experimental curves. As shown in figure 12, the predicted curves for a VW repulsive potential $A = -0.15$ and $A = -0.25$ remain very close from the one presented in the above subsection with $A = +0.2$. Similarly, a $C_2 z^{-2}$ or a $C_4 z^{-4}$ potential could approximately fit the experiments. As we shall see below, the quantitative predictions of atomic physics theory applied to VW interaction will justify the choice of an attractive z^{-3} potential to fit the experimental data.

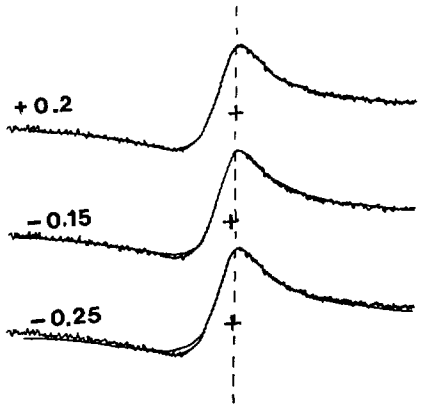

Fig. 12. — Comparison between attractive ($A > 0$) and repulsive ($A < 0$) VW potential for the fitting of an experimental curve (4-5 component of the D_2 transition at low pressure). The dashed vertical axis is the experimental line center of the atomic resonance (in volume spectroscopy). The crosses (+) provide origin and axis for the theoretical curves. Note that only $A = 0.2$ provides simultaneously a satisfactory agreement for far wings behavior and for resonance position. Discrepancies between $A = -0.15$ or $A = -0.25$ and the experimental curve is possible only due to an excellent signal to noise-ratio (better than in Fig. 9 because of a slightly larger irradiating intensity).

6. Theoretical estimates of the VW strength.

6.1 VW INTERACTION FOR Cs VAPOR/METAL INTERFACE. — For purposes of simplicity, we first consider the case of a Cs vapor interface with a perfect metal. The theoretical value of the VW strength is then governed by equations (1)-(3), while transition probabilities γ_{ij} and wavelengths of the virtual coupling are usually found in atomic data tables. However, the tabulated values are most often concerned only with radial integrals, so that some tensorial algebra is required to evaluate individual coupling with each component of a manifold, and to estimate the relative contribution of $\langle D_z^2 \rangle$. Because of this contribution, the van der Waals energy shift within a $|JM\rangle$ multiplet is in general not scalar, and contains a quadrupolar ($k = 2$) tensorial component. The energy shift is scalar only for $J = 0$ or $J = 1/2$ levels, for which $k = 2$ tensorial observable does not exist. A general analysis of the tensorial properties of surface-induced van der Waals shift, and their consequences on selective reflection will be published elsewhere.

In table II, we have listed, for the 4 levels to be considered ($6S_{1/2}$, $6P_{3/2}$, $7P_{1/2}$, $7P_{3/2}$), the dominant couplings to the various fine-structure energy levels [22], along with their respective wavelength and transition probability. In some cases, these values are directly provided in [23]. In other cases [24], it is extrapolated from the relative weight factor $(2J_i + 1) \begin{Bmatrix} J_i & L_j & S \\ L_i & J_j & 1 \end{Bmatrix}^2$ for a coupling cascading from $|j, L_j, J_j\rangle$ down to $|i, L_i, J_i\rangle$. This implies the following ratios to the overall transition probability :

— for $P_{1/2} \rightarrow S_{1/2}$. 1, $P_{3/2} \rightarrow S_{1/2}$. 1,
— for $S_{1/2} \rightarrow P_{1/2}$. 1/3, $S_{1/2} \rightarrow P_{3/2}$. 2/3,
— for $D_{3/2} \rightarrow P_{1/2}$. 5/6, $D_{3/2} \rightarrow P_{3/2}$. 1/6, $D_{5/2} \rightarrow P_{3/2}$. 1,
— for $P_{1/2} \rightarrow D_{3/2}$. 1, $P_{3/2} \rightarrow D_{3/2}$. 1/10, $P_{3/2} \rightarrow D_{5/2}$. 9/10.

To estimate the value of $\langle i | D^2 + D_z^2 | i \rangle$ — eventually averaged on the M_j magnetic sublevels, one needs to calculate its dependence on the $J_i \rightarrow J_j$ transition considered in the virtual dipole coupling :

$$\langle J_i M_i | D^2 + D_z^2 | J_i M_i \rangle = \sum_{M_j} \left\{ | \langle J_i M_i | D_x | J_j M_j \rangle |^2 + | \langle J_i M_i | D_y | J_j M_j \rangle |^2 + 2 | \langle J_i M_i | D_z | J_j M_j \rangle |^2 \right\} . \quad (12)$$

(i) For $J_j = J_i$

$$\langle i | D^2 + D_z^2 | i \rangle = \frac{3}{4} \hbar \gamma_{ij} \left(\frac{\lambda_{ij}}{2\pi} \right)^3 \left[1 + \frac{M_i^2}{J_i(J_i + 1)} \right] . \quad (13)$$

(ii) For $J_j = J_i + 1$

$$\langle i | D^2 + D_z^2 | i \rangle = \frac{3}{4} \hbar \gamma_{ij} \left(\frac{\lambda_{ij}}{2\pi} \right)^3 \left[1 + \frac{(J_i + 1)^2 - M_i^2}{(J_i + 1)(2J_i + 3)} \right] . \quad (14)$$

(iii) For $J_j = J_i - 1$

$$\langle i | D^2 + D_z^2 | i \rangle = \frac{3}{4} \hbar \gamma_{ij} \left(\frac{\lambda_{ij}}{2\pi} \right)^3 \left[1 + \frac{J_i^2 - M_i^2}{J_i(2J_i - 1)} \right] . \quad (15)$$

Table II. — *Theoretical contribution of the* $|i\rangle - |j\rangle$ *coupling to the* $|i\rangle$ *level* VW *shift.* λ_{ij} *. wavelength of the* $|i\rangle - |j\rangle$ *transition, the* (−) *sign stands for a lower* $|j\rangle$ *level. The transition probabilities* γ_{ij} *are from* [23], *or extrapolated from* [24] *when asterisked.*

i level	*j* level	λ_{ij} (μm)	γ_{ij} (10^6 s^{-1})	$\langle D^2 + D_z^2 \rangle$ contribution (kHz μm³)
$6S_{1/2}$	$6P_{1/2}$	0.894	28.6	0.82
	$6P_{3/2}$	0.852	32.4	1.60
$6P_{3/2}$	$6S_{1/2}$	(−) 0.852	32.4	0.80
	$7S_{1/2}$	1.47	11.4	0.72
	$8S_{1/2}$	0.795	3.6	0.06
	$5D_{3/2}$	3.61	0.11	0.21
	$5D_{5/2}$	3.49	0.94	1.86
	$6D_{3/2}$	0.921	2.66	0.08
	$6D_{5/2}$	0.918	15.2	0.71
	$7D_{3/2}$	0.699	1.22*	0.02
	$7D_{5/2}$	0.698	7.29*	0.25
	$8D_{3/2}$	0.622	0.62*	0.01
	$8D_{5/2}$	0.622	4.03*	0.06
$7P_{1/2}$	$6S_{1/2}$	(−) 0.459	2.12	0.01
	$7S_{1/2}$	(−) 3.096	3.52	4.19
	$8S_{1/2}$	3.919	1.38	3.32
	$9S_{1/2}$	1.944	0.45*	0.13
	$5D_{3/2}$	(−) 1.376	1.59	0.17
	$6D_{3/2}$	12.147	0.09	11.80
	$7D_{3/2}$	2.325	2.56*	1.77
	$8D_{3/2}$	1.655	1.11*	0.41
	$9D_{3/2}$	1.416	0.70*	0.16
$7P_{3/2}$	$6S_{1/2}$	(−) 0.455	2.97	0.01
	$7S_{1/2}$	(−) 2.931	4.05	4.08
	$8S_{1/2}$	4.218	2.62	3.93
	$9S_{1/2}$	2.014	0.89*	0.15
	$5D_{3/2}$	(−) 1.342	0.13	0.01
	$5D_{3/2}$	(−) 1.376	1.10	0.11
	$6D_{3/2}$	(−) 15.57	0.0086	1.21
	$6D_{5/2}$	(−) 14.60	0.063	11.75
	$7D_{3/2}$	2.438	0.348*	0.20
	$7D_{5/2}$	2.425	2.087*	1.79
	$8D_{3/2}$	1.705	0.223*	0.04
	$8D_{5/2}$	1.702	1.337*	0.40
	$9D_{3/2}$	1.452	0.161*	0.02
	$9D_{5/2}$	1.452	0.844*	0.15

In equations (13)-(15), the bracket, when averaged over M_i is always equal to 4/3. This reflects the relation $\langle D_z^2 \rangle = \frac{1}{3} \langle D^2 \rangle$. This implies that the average VW energy shift is 4/3 of the scalar shift when considering the coupling to lower levels. In the case of a dipolar coupling to upper levels ($E_j > E_i$), there is an additional weighting factor $(2J_j + 1)/(2J_i + 1)$ in equations (13)-(15), simply originating from the spontaneous emission factor when transitions coupling individual magnetic sublevels are considered. This adds :

(i) a factor 2 for $S_{1/2}$ (or $(P_{1/2})$ levels coupled to upper $P_{3/2}$ (or $D_{3/2}$) levels ;
(ii) a factor 1/2 or 3/2 for a $P_{3/2}$ level coupled to upper $S_{1/2}$ or $D_{5/2}$ levels, respectively.

With the above considerations, and with atomic data given in table II, one easily estimates the rspective VW attraction coefficients, when neglecting the effect of the hyperfine structure :

2.4 kHz μm^3 for the $6S_{1/2}$ level, 4.8 kHz μm^3 for the $6P_{3/2}$ level, 22.0 kHz μm^3 for the $7P_{1/2}$ level, 23.9 kHz μm^3 for the $7P_{3/2}$ level.

One notes that in all cases, the overall VW spectral shift is a red-shift, as the VW attraction exerted on the ground state always remains smaller than the one exerted on an excited atom. If the ground state contribution is not negligible in the overall red shift predicted for the D_2 line (2.4 kHz μm^3) [25], it provides only a small contribution to the VW shift predicted for the blue transitions $6S_{1/2}$-$7P_{1/2}$ and $6S_{1/2}$-$7P_{3/2}$. This is clearly related with the large polarizability of highly excited states, and fully justifies to go to excited transitions for observing strongly VW distorted lineshapes.

More extensive calculations would be needed to evaluate the effect of the hyperfine structure. However, it should be noticed that no changes are expected for $J = 1/2$ levels (hence, notably in the calculation of the $6S_{1/2}$ and $7P_{1/2}$ VW shift which is purely isotropic). Also a P level is shifted by a D level in a quasi isotropic manner (for a P-D coupling, one has $\langle m = 1 | D^2 + D_z^2 | m = 1 \rangle / \langle m = 0 | D^2 + D_z^2 | m = 0 \rangle = 13/14 \approx 1$), and one notices from table II that the $6P_{3/2}$ and $7P_{3/2}$ levels are the more strongly shifted by neighboring $D_{5/2}$ levels (rather than by neighboring $S_{1/2}$ levels, whose VW shift contribution is much more anisotropic). It seems then reasonable to neglect, in a first approach, the variations of the VW attraction with respect to the various hyperfine components. Let us recall also that experimental sensitivity did not permit to observe any variation of the surface effect with the hyperfine component.

6.2 EFFECTS RELATED WITH THE DIELECTRIC NATURE OF THE INTERFACE. — In a simple approach, when a perfect metal interface is replaced by a transparent dielectric medium, the electrostatic image is attenuated by a factor $[(\varepsilon - 1)/(\varepsilon + 1)]$, where ε is the dielectric permittivity. Taking for sapphire $\varepsilon = n^2 = (1.76)^2$ and neglecting dispersion effects, one would predict a VW shift attenuated by a factor 0.51 leading to a prediction of 1.2 kHz μm^3 red shift for the Cs D_2 line, 10 kHz μm^3 for $6S_{1/2}$-$7P_{1/2}$ and 10.8 kHz μm^3 for $6S_{1/2}$ -$7P_{3/2}$ transition. These values are typically a factor of 2 below our experimental determination. On the other hand, a satisfactory agreement is obtained with this simple approach for the relative comparison between glass ($\varepsilon = n^2 = (1.5)^2$) and sapphire, which fully justifies the $9/13\ A_{\text{glass}}/A_{\text{sapphire}}$ ratio observed on the blue transition.

However, a severe limit to the validity of this treatment lies in the fact that the strongest couplings responsible for VW attraction are in the long wavelength range. For the $6P_{3/2}$ level, the major contribution to the VW shift lies in the 3.49 μm coupling with the $5D_{5/2}$ level, while for the 7P level, the most notable contribution originates in the coupling with the 6D level, corresponding to a transition at 15 μm ($7P_{3/2}$ level) or 12 μm ($7P_{1/2}$ level). If a sapphire window is still transparent at 3.5 μm, absorption becomes

important at 5-6 μm, so that simple corrections to the estimate for metallic interface are quite dubious for the VW shift on the blue transition.

An extra amount of theoretical work remains needed and is in progress to deal with the problem of a multi level-atom near a partly absorbing dielectric. Let us note that in our problem, the dielectric properties — dispersion and absorption — are observed in a region of transparency, and are in a way probed through some frequency filtering originating in the quantum mechanical nature of the atomic vapor. Also, in the experiments presented above, there is no effective monitoring of the real surface state, and one could imagine that a Cs metallic coating has deposited on the window. This could seem to provide a closer expectation value of the VW shift, but difficulties arise from the significant difference between glass and sapphire windows, and from the fact that off-resonance reflectivity at 0.85 μm or at 0.45 μm clearly provides the values for reflection on an uncoated window.

7. Conclusion.

In conclusion, our work proves experimentally and theoretically that (FM) selective reflection spectroscopy is an adequate tool for observing the signature of long-range interaction exerted by a surface on an atomic vapor. Direct inversion of the surface interaction potential from the SR lineshapes would be a difficult task with respect to the double spatial averaging typical of the SR technique. However, it has been shown that, from a single lineshape, it is possible to discriminate to some extent between various shapes of potential. The key point establishing the van der Waals nature of the observed surface attraction is the remarkable agreement between experimental distorted lineshapes and theoretical predictions governed by a single parameter. This agreement is consistent with the pressure studies as well as with the angular studies, and is systematic for the various hyperfine components.

Moreover, the measured strength of this VW attraction is quite compatible, for both types of transition (D_2 line and weak VW regime, second resonance line and strong VW regime) with the values predicted when taking into account the transition probabilities provided by the atomic theory. Several causes could explain the slight discrepancy (by a factor less than 2) between experimental and predicted VW strength : in particular, the hyperfine structure is ignored in the calculation and the dielectric absorption at some of the virtual transitions wavelength is not taken into account (in particular in the case of the second resonance line). Also, the very nature of the surface is not accurately known and metallic or impurity layers could cover it, although the glass/sapphire comparison should rule this out as a dominant mechanism. Besides, it seems unlikely that a residual contribution of the oscillating resonant interaction with the surface (whose amplitude never exceeds 0.25 γ, see [12]) behaves similarly to an extra VW contribution. Also, for the blue transition, several channels of spontaneous emission are opened, and this should decrease the relative magnitude of the resonant term.

One should outline that the (FM) SR spectral technique provides for the first time information on the VW attraction exerted on a short lifetime excited level. As proved by the calculation, and by the comparison between the two series of experiments (λ = 852 nm and λ = 455 nm), the excited level provides the dominant contribution to the VW interaction. Also, as SR spectroscopy is a coherent technique, intrinsically sensitive to the difference between level-dependent surface attraction, one can even expect specific quantum features notably coupling internal and external degrees of freedom, and related with the quantized motion in a state-dependent potential. If these quantum effects, which exceed the scope of our model for SR spectroscopy in the presence of a surface potential, are not observed in our experiments, this has to be attributed to the heavy mass of Cs and to the relatively large width of the velocity selection by the FM technique. Because of this coherent nature of the SR

technique, and of the dominant contribution of the excited state VW attraction, singling out the ground state surface interaction can seem a challenge. However, such an information, which could discriminate between various sub-level contributions and should be no longer limited by an optical transition linewidth, could be delivered by various extensions of linear SR spectroscopy to double resonance spectroscopy, including addition of a tunable microwave coupling, and nonlinear Raman-type SR spectroscopy.

Finally, the observation of an interaction exerted by a dielectric surface is also a stimulating point. Indeed, the theory is much less developed than for the case of a perfect metal, and one can think about SR spectroscopy of a known vapor at a dielectric interface as a new technique to investigate dielectric properties, which would be frequency selective at the frequency of the virtual transitions of the vapor. Recent works using dielectric structure for photonic crystals should also increase the interest in studying the optical-range surface interaction of a dielectric medium [26].

Acknowledgments.

We thank C. Brechignac, Director of Laboratoire Aimé Cotton, for her hospitality and for having provided us with the blue laser system. We thank G. Flory for having kindly filled the Cs cells.

Appendix A

Red shift and blue shift : repulsive potential and propagation effect in an optically dense medium.

It can seem astonishing that an overall repulsive VW interaction, associated with an increase in the transition energy, is predicted to be responsible for a red-shift in the slightly distorted (FM) SR lineshape (for $|A| \ll 1$) (see Fig. 2). This results from the spatial averaging involved in SR spectroscopy, which mixes absorption and dispersion through a phase factor.

A simple interpretation of this phenomenon can be given by considering the case of SR spectroscopy of motionless atoms evolving in a potential.

Indeed, with a repulsive VW potential, one similarly predicts a red-shifted slightly distorted ($|A| \ll 1$) SR lineshape for motionless atoms (see Fig. A1). As already mentionned in 3.1,

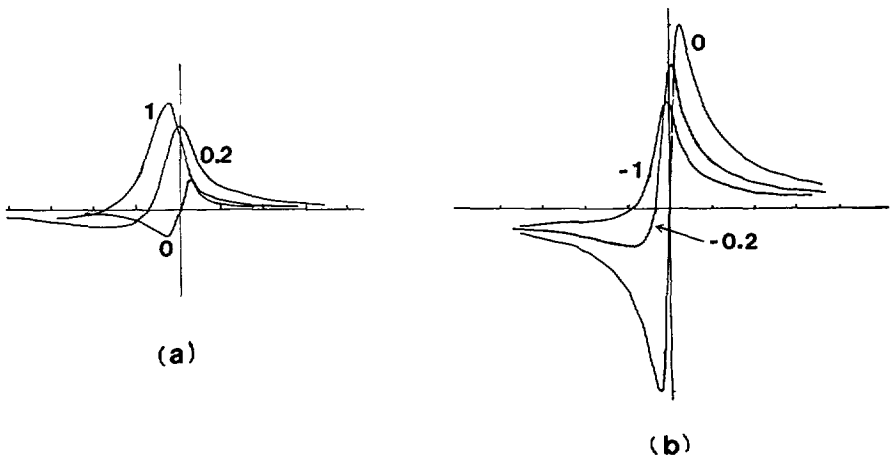

Fig. A1. — Theoretical lineshapes for SR spectroscopy of motionless atoms in the presence of a weak VW attractive (a) or repulsive (b) potential. Values of A as indicated.

equation (7), along with $\Delta R \propto \mathrm{Re}\,\Delta\varepsilon_r$, easily shows that if the induced dipole $p(z)$ is a constant $p(z) = p_0$ (i.e. in the absence of surface interaction and of absorption along the propagation), the SR signal is just proportional to the dispersion of the medium $\mathrm{Re}\,p_0$. This is because the absorptive contribution (proportional to $\mathrm{Im}\,p_0$), which is maximum at $z = q\lambda/4$ (q : integer) and minimum at $z = (q + 1/2)\,\lambda/4$, totally vanishes in the spatial averaging. Spectrally, the line center for the dispersive SR signal is obtained just on resonance, when the dispersion is zero and the absorption is maximum. Let us now consider a surface interaction, whose combined strength and spatial extension make the surface-induced shift negligible everywhere but for $z \ll \lambda/4$. Hence, the SR signal for an irradiation exactly centered on the atomic resonance is no longer zero. Indeed, in the vicinity of the surface, the absorption contribution is decreased because the resonance is shifted for atoms neighboring with a surface and there is no more a balance in the spatial averaging of this absorptive contribution. This residual absorptive contribution makes the SR lineshape asymmetric and shifts its zero. The important point to notice is that, at least for a small enough surface interaction potential, the sign of this absorptive contribution at atomic line center, which determines the sign of the SR lineshape shift, is independent of the attractive or repulsive nature of the potential : in both cases, the absorption contribution is off-resonance near the surface. Hence, we have no surprise if VW repulsion (blue-shifting surface interaction) implies a red-shift of the SR spectrum, as does a VW attraction.

In a similar manner, one can understand that for non negligible atomic densities, i.e. when attenuation over λ of the incident irradiation is not entirely negligible one predicts a blue shift of the SR lineshape. This result, predicted in a complete calculation taking into account atomic motion [14], also appears in a simplified model for motionless atoms when taking into account a phenomenological non resonant absorption coefficient α_0, so that equation (7) now becomes :

$$\Delta\varepsilon_r = \frac{ik}{(n_1 + 1)} \int_0^\infty p_0 \exp(-\alpha_0 z) \exp(2ikz)\, dz \qquad \text{(A1)}$$

with $p_0 \propto 1/\left[-(\omega - \omega_0) - i\,\frac{\gamma}{2}\right]$ for a standard two-level resonant system. The blue shift and asymmetry is once again explained by the residual absorptive contribution (related with $\mathrm{Im}\,p_0$) and is approximately equal to $\alpha_0\,\gamma/4\,k$, as results from unbalance in the spatial averaging in equation (A1). However, for irradiation resonant with atomic linecenter, the absorptive contribution is now enhanced near the surface, instead of being attenuated by resonance-shifting surface interaction. It is thus no surprise if a blue shift (instead of a red one) is predicted when a weak, but non negligible absorption is considered.

Finally, as pressure shifts were measured in the two series of experiments, it would be interesting to determine if interatomic collisional processes are the dominant origin of this shift, or if it is an optical density artefact related with the SR technique itself. The extension of Schuurmans theory in an optically dense medium, to include the effect of surface interaction and in the Doppler-free FM technique is still in progress. Anyhow, as the Doppler-broadened absorption coefficient varies much more slowly than the FM SR signal, and as a motionless model can provide satisfactory qualitative pictures, one can expect to evaluate the order of magnitude of the density-related blue shift from a motionless SR theory. With the effectively measured absorption coefficient (from $6S_{1/2}$ ($F = 4$) state) : $\alpha \approx 1.5 \times 10^{-11}\,\mathrm{cm}^{-1}/\mathrm{at.cm}^{-3}$ for $\lambda = 852$ nm, and $\alpha \approx 2.5 \times 10^{-13}\,\mathrm{cm}^{-1}/\mathrm{at.cm}^{-3}$ for $\lambda = 455$ nm, one predicts in this simple model a density-induced blue-shift of $4 \times 10^{-10}\,\mathrm{Hz/at.cm}^{-3}$ for $\lambda = 852$ nm and of $3 \times 10^{-12}\,\mathrm{Hz/at.cm}^{-3}$ for $\lambda = 455$ nm (one takes for γ the observed value in the limit of low densities i.e. respectively 8 MHz and 6 MHz for 852 nm and 455 nm). These values are

smaller than the measured pressure shifts by an order of magnitude for $\lambda = 852$ nm, and by a factor 1 000 for $\lambda = 455$ nm. Although atomic motion over numerous wavelengths (typical of a quasi non resonant absorption, e.g. associated with the Doppler-broadened absorption on a neighboring component) may sensitively increase these blue shifts, one can reasonably expect that collisional effects are the dominant phenomenon explaining the observed pressure shift rather than cell opacity. For the blue transition, the very good agreement with theory for an optically thin vapor obtained in the systematic study of the lineshape should confirm that optical density effects remain negligible in all of our work, as the SR lineshapes in the presence of FM should be modified and not only shifted when absorption of the irradiation is taken into account.

References

[1] Oria M., Chevrollier M., Bloch D., Fichet M. and Ducloy M., *Europhys. Lett.* **14** (1991) 527.

[2] Chevrollier M., Bloch D., Rahmat G. and Ducloy M., *Opt. Lett.* **16** (1991) 1879.

[3] Akul'shin A. M., Celikov A. A., Sautenkov V. A., Vartanian T. A. and Velichanskii V. L., *Opt. Commun.* **85** (1991) 21.

[4] Ducloy M. and Fichet M., *J. Phys. II France* **1** (1991) 1429.

[5] Raskin D. and Kusch P., *Phys. Rev.* **179** (1969) 712 ;
Shih A., *Phys. Rev. A* **9** (1974) 1507.

[6] Shih A., Raskin D. and Kusch P., *Phys. Rev. A* **9** (1974) 652 ;
Shih A. and Parsegian V. A., *Phys. Rev. A* **12** (1975) 835.

[7] Anderson A., Haroche S., Hinds E. A., Jhe W. and Meschede D., *Phys. Rev. A* **37** (1988) 3594.

[8] Meschede D., Jhe W. and Hinds E. A., *Phys. Rev. A* **41** (1990) 1587 and references therein.

[9] Kleppner D., *Phys. Rev. Lett.* **47** (1981) 233 ;
Goy P., Raimond J. M., Gross M. and Haroche S., *Phys. Rev. Lett.* **50** (1983) 1903 ;
Jhe W., Anderson A., Hinds E. A., Meschede D., Moi L. and Haroche S., *Phys. Rev. Lett.* **58** (1987) 666 ;
Heinzen D., Childs J. J., Thomas J. E. and Feld M. S., *Phys. Rev. Lett.* **58** (1987) 1320.

[10] Casimir H. G. and Polder D., *Phys. Rev.* **73** (1948) 360.

[11] Kasevich M., Moler K., Riis E., Sunderman E., Weis D. and Chu S., in Atomic Physics 12, Zorn and Lewis Eds. (American Institute of Physics, New York, 1991) pp. 47-57 ;
Hinds E. A., Sukenik C. I., Boshier M. G. and Cho D., *ibid.* (1991) pp. 283-287 ;
Lundeen S. R., *ibid.* (1991) pp. 288-309.

[12] Hinds E. A. and Sandoghdar V., *Phys. Rev. A* **43** (1991) 398.

[13] Wood R. W., *Philos. Mag.* **18** (1909) 187.

[14] Schuurmans M. F. H., *J. Phys. France* **37** (1976) 469.

[15] Nienhuis G., Schuller F. and Ducloy M., *Phys. Rev. A* **38** (1988) 5197.

[16] The « metallic reflection » predicted in dense vapor resonantly irradiated by a strongly saturating beam by Roso Franco L. [*Phys. Rev. Lett.* **55** (1985) 2149] also corresponds to a rapid variation of $p(z)$ on a distance smaller than λ. Nevertheless, the discontinuity no longer occurs at the surface, but in the bulk. SR spectroscopy would thus essentially probe this narrow region of the bulk, where propagation suddenly stops down.

[17] Woerdman J. P. and Schuurmans M. F. H., *Opt. Commun.* **16** (1975) 248.

[18] Akul'shin A. M., Velichanskii V. L., Zibrov A. S., Nikitin V. V., Sautenkov V. V., Yurkin E. K. and Senkov N. V., *JETP Lett.* **36** (1982) 303.

[19] Alekseev V. A. at Lebedev Physics Institute (Moscow) has shown in a perturbation expansion for very weak VW interaction that VW repulsion would produce a red-shifted lineshape (private communication).

[20] ORIA M., BLOCH D. and DUCLOY M., in Laser Spectroscopy IX, M. S. Feld *et al.* Eds. (Academic Press, New York, 1989) pp. 51-53.

[21] For these experiments, the measured temperature was 180 °C as indicated in reference [2] (Fig. 4) corresponding to a 30 mtorr pressure, and not to 60 mtorr as wrongly indicated in [2].

[22] MOORE C. E., Atomic Energy levels **III,** NSRDS-NBS 35 (Washington D. C., 1971) pp. 124-128.

[23] HEAVENS O. S., *J. Opt. Soc. Am.* **51** (1961) 1058.

[24] LINDGARD A. and NIELSEN S. E., in Atomic Data and Nuclear Tables **19** (Academic Press, 1977) pp. 533-633.

[25] In a similar manner, one shows that the overall red shift on the D_1 line is only 1.6 kHz μm^3, so that the ground state contribution is more than half the one of the resonant state $6P_{1/2}$.

[26] YABLONOVITCH E., GMITTER T. J., MEADE R. D., RAPPE A. M., BRUMMER K. D. and JOANNOPOLOUS J. D., *Phys. Rev. Lett.* **67** (1991) 3380.